HHS Public Access

Author manuscript

Nat Struct Mol Biol. Author manuscript; available in PMC 2009 May 01.

Published in final edited form as:

Nat Struct Mol Biol. 2008 November ; 15(11): 1152–1159. doi:10.1038/nsmb.1507.

Activation of Slo1 BK channels by Mg^{2+} coordinated between the voltage sensor and the RCK1 domains

Huanghe Yang, **Jingyi Shi**, **Guohui Zhang**, **Junqiu Yang**, **Kelli Delaloye**, and **Jianmin Cui**

Department of Biomedical Engineering and Cardiac Bioelectricity and Arrhythmia Center, Washington University, 1 Brookings Drive, St. Louis, MO 63130, USA

Abstract

The voltage sensor domain (VSD) and the ligand sensor (cytoplasmic domain) of BK channels synergistically control channel activities, thereby integrating electrical and chemical signals for cell function. Studies show that intracellular Mg^{2+} mediates the interaction between these sensory domains to activate the channel through an electrostatic interaction with the VSD. Here we report that Mg^{2+} binds to a site that consists of amino acid side-chains from both the VSD (Asp99 and Asn172) and the cytoplasmic domain (Glu374 and Glu399). For each Mg^{2+} binding site the residues in the VSD and those in the cytoplasmic domain come from neighboring subunits. These results suggest that the VSD and the cytoplasmic domains from different subunits may interact during channel gating, and the packing of VSD or the RCK1 domain to the pore in BK channels differ from that in Kv1.2 or MthK channels.

INTRODUCTION

Many ion channels are assembled from modular elements1, in which a sensory module to specific stimuli, such as voltage, ligand binding, post-translational modification, and accessory protein association, usually covalently links to the ion conduction pore and thereby regulates its opening and closing. The direct interaction between the channel pore and various sensory modules in a number of ion channels, such as the membrane-spanning voltage sensor of Kv channels2, the cytoplasmic Ca^{2+} sensor of MthK channels3, and the extracellular ACh binding domain of ACh receptors4, has been proposed as a key step for channel activation. However, how stimuli alter the interaction among different sensors to promote channel activation is still not clear. Here we study the Slo1 large conductance, voltage- and Ca^{2+}-activated K^+ (BK) channel to address this question, because the BK channel has a distinct voltage sensor domain (VSD) and a cytoplasmic ligand-binding domain to separately sense membrane voltage and intracellular ligands5-13, and previous studies have shown that the two sensory domains interact during channel gating14.

Address Correspondence to: Jianmin Cui, Department of Biomedical Engineering, 1 Brookings Drive, Washington University, St. Louis, MO 63130, Tel: (314)-935-8896, Fax: (314)-935-7448, Email: jcui@biomed.wustl.edu.

AUTHOR CONTRIBUTIONS H.Y., J.S., and J.C. designed the research; H.Y., J.S., G.Z., J.Y. and K.D. performed the experiments; H.Y., G.Z. and J.Y. analyzed the data; H.Y. and J.C. wrote the paper.

An abstract of this work has been presented in the 52nd Annual Meeting of Biophysical Society.

BK channels are activated by voltage, intracellular Ca^{2+} and Mg^{2+} (Fig. 1 a, b) 5-7, and participate in various physiological functions, such as muscle contraction, neural transmission and hearing7,15-18. Both sequence homology and experimental evidence suggest that the structure of the VSD in BK channels may resemble that of other Kv channels19, while the cytoplasmic domain of BK channels may adopt a similar structure as that of the MthK channel3,8,12,14,20,21. Previous studies on Mg^{2+}-dependent activation of BK channels have revealed structural details that are important for BK channel function. Particularly, two acidic amino acids (Glu374 and Glu399) in the cytoplasmic RCK1 domain of BK channel may contribute to Mg^{2+} coordination12-14,22; removal of the side chain carboxylate groups from these two residues completely abolishes Mg^{2+} sensing. These residues in the cytoplasmic domain are located close to the C-terminus of the transmembrane segment S4, enabling the bound Mg^{2+} to engage in an electrostatic interaction with the voltage-sensing residue Arg213 at the C-terminus of S414 (Fig. 1c).

To further understand the mechanism of Mg^{2+}-dependent activation of BK channels and explore the structural basis of the interaction between the VSD and the cytoplasmic domains of mouse Slo1 (mSlo1), we studied the composition of the Mg^{2+} binding site. As a “hard” (closed-shell) divalent cation, Mg^{2+} is dominantly coordinated by six “hard” oxygen atoms from the side chains of oxygen-containing residues, main chain carbonyl groups in proteins, or water molecules (Fig. 1c, inset)23. Besides two putative Mg^{2+} coordinates contributed by the carboxylate groups from Glu374 and Glu399 (Fig. 1d), four additional oxygen ligands are required for Mg^{2+} binding. In this study, we identified two more amino acid side chains, Asp99 and Asn172, in the voltage sensor domain that may also contribute to Mg^{2+} coordination. Interestingly, our results indicate that Asp99 and Asn172 from the VSD of one subunit may form the Mg^{2+} binding site with Glu374 and Glu399 from the cytoplasmic domain of a neighboring subunit. Such an inter-domain and inter-subunits formation of the Mg^{2+} binding site reveals a particular structural alignment of the VSD and the cytoplasmic domain and indicates that the two domains from different subunits may interact during BK channel gating.

RESULTS

Ala-scan in the cytoplasmic domain of BK channels

Figure 1c shows the structure of the cytoplasmic RCK1 domain of MthK, which has been proposed as the structural model for the cytoplasmic domain of BK channels3. The putative Mg^{2+} coordinates Glu374 and Glu399 are located at the N-terminus of the RCK1 domain (the AC region, colored cyan in Fig. 1c). Since Glu374 and Glu399 are located at the top surface of the cytoplasmic domain, if any side chain from the cytoplasmic domain other than these two residues also contributes to Mg^{2+} coordination, it should be located in the AC region. To identify such a residue, we made an Ala-scanning of all the residues with oxygen-containing side chains in the AC region. If any of these residues contributes to Mg^{2+} coordination, the substitution of its side chain with the methyl group of Ala would abolish or substantially reduce the Mg^{2+}-induced shift of the *G-V* relation (Fig.1b). However, except for the mutations of Glu374 and Glu39912, we did not find any Ala mutation that markedly reduced Mg^{2+} sensing (Fig. 1d, other mutational results have been published previously12).

Therefore, Glu374 and Glu399 are the only two putative Mg^{2+} coordinates in the cytoplasmic AC region. Here and in all other figures, the bars represent observed *G-V* shifts induced by 10 mM $[Mg^{2+}]_i$ subtracting 14.0 mV due to Mg^{2+} binding to another low affinity Mg^{2+} site24.

D99A prevents Mg^{2+} binding

We then examined if the transmembrane (TM) domain contains side chains that may contribute to Mg^{2+} coordination. Since mSlo1 (mouse) and dSlo (drosophila) channels show similar Mg^{2+} sensitivity, 45 oxygen-containing residues in the TM domain conserved between these two species and potentially facing cytosol were mutated into amino acids that contain no side chain oxygen (Fig. 2a, red and blue colors). Among these mutations, only D99A, which is located in the C-terminus of the S0-S1 linker (Fig. 1c, 2a), completely abolishes the *G-V* shift induced by 10 mM $[Mg^{2+}]_i$; two other mutations, N172A and Y336A, substantially reduce the *G-V* shift (Fig. 2b-d).

Recent studies showed that Mg^{2+} activates the channel by an electrostatic interaction with Arg213 in S4 after binding to the channel14. Therefore, mutation D99A could eliminate Mg^{2+} sensitivity by either a direct destruction of the Mg^{2+} binding site to prevent Mg^{2+} binding or an alteration of the conformation to prevent the interaction between the bound Mg^{2+} and Arg213. To distinguish these two possibilities, we examined whether D99A also abolishes the effect of a positive charge covalently added to the vicinity of the Mg^{2+} binding site. Previous studies show that Gln397 is located close to the Mg^{2+} binding site12,22. A positive charge covalently added to position 397 by modifying Q397C with MTSET(+) shifts *G-V* relation to more negative voltages (Fig. 2e) because the charge also interacts with Arg213 electrostatically to activate the channel, mimicking the effects of Mg^{2+} on the WT channel14. If D99A alters the conformation of the channel to prevent the interaction between the bound Mg^{2+} and Arg213, it should also abolish the effects of MTSET(+) modification of Q397C. However, as shown in Figure 2e, in the presence of D99A, the modification of Cys397 by MTSET(+) still shifted *G-V* relation by -51.7±1.6 mV, comparable with the shift in the absence of D99A (-66.5±1.8 mV). These results indicate that D99A does not markedly alter the electrostatic interaction between the VSD and the positive charge around the Mg^{2+} binding site.

Next, we measured the effect of D99A on gating currents with and without 10 mM $[Mg^{2+}]_i$. The off-gating current (I_{gOFF}) is derived from the return of the voltage sensor from the active state to the resting state when most channels are open, while the on-gating current (I_{gON}) is the result of the movement of the voltage sensor from the resting state to the active state when channels are closed14,25-27. Our recent studies demonstrated that Mg^{2+} affects WT I_{gOFF} through an electrostatic interaction with Arg213 in S4 primarily when the channel is open14. For WT channels, 10 mM $[Mg^{2+}]_i$ reduces the amplitude and the decay rate of the I_{gOFF} but does not noticeably affect the I_{gON} (Fig. 2f and Supplementary Fig. 1a). However, D99A almost abolishes the effect of Mg^{2+} on I_{gOFF} (Fig. 2f, g), indicating that S4 can no longer sense Mg^{2+}. Since D99A does not affect the ability of S4 to sense a positive charge covalently added to the vicinity of the Mg^{2+} binding site (Fig. 2e), this result indicates that Mg^{2+} can no longer bind to the site to interact with S4. Similar results were obtained with

the mutation E399N, which destroys Mg^{2+} binding at the Glu374/Glu399 site (Supplementary Fig. 1). Taken together, mutation D99A destroys Mg^{2+} binding to the Glu374/Glu399 site.

Asp99 is part of the Mg^{2+} binding site

Why does D99A abolish Mg^{2+} binding? The simplest hypothesis is that the carboxylate group on the side chain of Asp99 provides another Mg^{2+} coordinate. For this to be true, we should expect that 1) Asp99 is close to residues Glu374/Glu399 in the cytoplasmic domain so that they can be part of the same Mg^{2+} binding site; and 2) the oxygen on the side chain of Asp99 is required for Mg^{2+} binding.

To examine the spatial relationship between Asp99 and Glu374/Glu399, we made a double mutation D99C Q397C and examined whether a disulfide bond could form between these two Cys residues. Since the C_β- C_β distance between two Cys residues in a disulfide bond is between 2.9 to 4.6 Å28 and Gln397 is close to Glu39912,14,22, a disulfide bond between Cys99 and Cys397 would indicate that Asp99 and Glu374/Glu399 are located within the dimension of a Mg^{2+} binding site. Figure 3a and b show that the treatment of D99C Q397C channels with 10 mM DTT induced a shift of -15.0±1.6 mV in the *G-V* relationship. This shift is significant compared with the DTT effect on WT, D99C and Q397C channels ($p<0.001$), suggesting a spontaneous disulfide bond formation between Cys99 and Cys397, which is subsequently reduced by DTT.

To further demonstrate the existence of this disulfide bond, we treated D99C Q397C mutant channels with 200 μM MTSET(+). MTSET(+) treatment of Q397C channels induces a -66.5±1.8 mV leftward shifts of the *G-V* relationship in the absence of Mg^{2+} (Fig. 2e)14. A disulfide bond between Cys99 and Cys397 would protect the thiol group on residue 397, which would be then no longer available for MTSET(+) to modify, resulting in no MTSET(+)-induced *G-V* shift. Consistent with this prediction, MTSET(+) did not show any effect on the *G-V* relationship of the D99C Q397C channel (Fig. 3c, d). The absence of the MTSET(+) effect is not due to the mutational effect of Asp99, because D99A Q397C channels still can sense MTSET(+), while single mutant D99C is insensitive to MTSET(+) (Fig. 2e and 3d). The sequential treatment with 10 mM DTT and followed by 200 μM MTSET(+) resulted in a partial recovery of the MTSET(+) effect (-24.5±2.0 mV, Fig. 3c, d), further indicating the existence of the disulfide bond between Cys99 and Cys397. This partial recovery of the MTSET(+) effect suggests that the disulfide bond between Cys99 and Cys397 is broken by 10 mM DTT only in a fraction of the channels, possibly due to the fast reformation of the disulfide bond. Such a phenomenon suggests that Cys99 and Cys397 are located very close to allow a fast, spontaneous formation of the disulfide bond. A similar phenomenon has been reported in the study of the cyclic-nucleotide gated channel29. Therefore, these experiments indicate that Asp99 in the S0-S1 loop is located spatially close to Gln397, and the Glu374/Glu399 site, in the cytoplasmic domain.

To test the role of side chain oxygen of residue 99 on Mg^{2+} sensing, we mutated Asp99 to amino acids with various side chains (Fig. 4a). Mg^{2+} sensing, but not voltage or Ca^{2+} sensing, is highly correlated with the side chain properties of residue 99 (Fig. 4a, b). Similar to D99A, all the mutations that remove side chain oxygen (D99C, D99W, D99R and D99K)

completely abolished Mg^{2+} sensitivity, while the mutations that preserve oxygen with carbonyl or carboxylate groups (D99Q, D99N and D99E) retained partial Mg^{2+} sensitivity. Among these mutations, D99E channels showed higher Mg^{2+} sensitivity than D99Q and D99N channels. This is consistent with the higher preference of carboxylate group over carbonyl group on Mg^{2+} binding23. To the contrary, none of the mutations noticeably altered the *G-V* shifts induced by 100 μM $[Ca^{2+}]_i$ (Fig. 4a) or the equivalent gating charge *z* (Fig. 4b), indicating that the mutational effect of residue 99 is specific to Mg^{2+} sensing of the BK channel. Therefore, the oxygen on its side chain is essential for Mg^{2+} binding. Based on the spatial proximity, the mutational effects on Mg^{2+} sensing and Mg^{2+} binding, as well as the fact that Asp99 is conserved among BK channels from different species (Fig. 4c), we conclude that Asp99 from the VSD and Glu374/Glu399 from the cytoplasmic domain form a putative inter-domain Mg^{2+} binding site.

Asn172 also participates in Mg^{2+} binding

In addition to D99A, two other mutations, N172A in the S2-S3 loop and Y336A in the linker connecting S6 to the cytoplasmic domain, substantially reduced Mg^{2+} sensing of the channel (Fig. 2b). To investigate whether these two residues contribute to Mg^{2+} coordination, we first mutated them to basic residues (positively charged) (Fig. 5a, b). We have shown that mutating a putative Mg^{2+} ligand, Glu374, Glu39922, or Asp99 (Fig. 4a), to basic residues completely abolishes Mg^{2+} sensitivity of the channel due to the destruction of Mg^{2+} coordination. On the other hand, if a residue (for example, Gln397) is in the vicinity of the Mg^{2+} binding site but is not a Mg^{2+} coordinate, positively charged mutations of this residue (ie. Q397R/K) reduce but cannot abolish Mg^{2+} sensitivity; while negatively charged mutations (ie. Q397D/E) increase Mg^{2+} sensitivity 22 (Fig. 5b) . The change of Mg^{2+} sensitivity by these mutations might be due to the conformational change of the Mg^{2+} binding site and/or the electrostatic interactions between Mg^{2+} and the charges. However, when we tested charged mutations of Tyr336, we found that both Y336R and Y336E reduced Mg^{2+} sensitivity. But none of them abolished or enhanced Mg^{2+} sensitivity (Fig. 5b). These phenomena indicate that Tyr336 may not be part of the Mg^{2+} binding site, nor close enough to the binding site to affect Mg^{2+} binding through electrostatic interactions. Rather, the reduction of Mg^{2+} sensitivity is likely due to allosteric effects.

In contrast, N172R and N172K completely abolish Mg^{2+} sensing (Fig. 5a, b), while N172D and N172E increase Mg^{2+} sensitivity. Other mutations of Asn172 reduce Mg^{2+} sensitivity (Fig. 5a, b). Does Asn172 contribute to Mg^{2+} coordination, or alternatively, is it simply close to the Mg^{2+} binding site such that adding a positive charge on its side chain completely excludes Mg^{2+} binding, while adding a negative charge attracts Mg^{2+} to bind (Fig. 5c, inset)? To answer this question, we tested whether N172D can rescue Mg^{2+} sensitivity that is abolished by the mutations of the putative Mg^{2+} binding residues (D99A, E374A or E399N) (Fig. 5c). If Asn172 is part of the Mg^{2+} binding site, the carboxylate group of N172D may be able to substitute the loss of one carboxylate group induced by single mutations D99A, E374A or E399N, to coordinate Mg^{2+}. Consistent with this hypothesis, the double mutant channels containing N172D show substantially larger Mg^{2+} sensitivity than these single mutant channels (Fig. 5c), indicating that N172D can substitute these residues and rescue Mg^{2+} binding. However, N172D cannot rescue any Mg^{2+}

sensitivity from the combinatorial effect of E374A and E399R, which removes two carboxylate groups from the original Mg^{2+} binding site, suggesting that N172D can only compensate for one lost carboxylate group. Contrary to the effect of N172D, adding a carboxylate group on residue 397 can not rescue any Mg^{2+} sensitivity when the side chain carboxylate group of Glu374 was removed (Fig. 5c, E374A Q397E). Thus, Asn172 plays a different role than Gln397 on Mg^{2+} binding. These results suggest that the increase of Mg^{2+} sensitivity by N172D/E or the elimination of the Mg^{2+} sensitivity by N172R/K cannot be simply attributed to the electrostatic interaction between Mg^{2+} and the charge on residue 172. Instead, the carboxylate or carbonyl group on the side chain of residue 172 may contribute to Mg^{2+} coordination.

Mg^{2+} binding sites are formed between neighboring subunits

It has been proposed that the structures of the VSD and the cytoplasmic RCK1 domain of BK channels resemble that of the VSD of Kv1.2 channels19 and the RCK domain of MthK channels3,12,14,22, respectively. However, it is not clear how these sensory domains align with each other in BK channels. In Figure 6a we combine the structures of Kv1.2 (PDB ID: 2A79)30 and MthK (PDB ID: 1LNQ)3 by aligning the selectivity filter of the two channels, which provides an opportunity to examine the packing of different structure domains in the BK channel.

Figure 6a shows that, if the VSD and the RCK1 domain of BK channels pack against the pore domain similarly as that of Kv1.2 and MthK, the VSD would be located just above the RCK1 domain from the same subunit. Such a model would predict that all four Mg^{2+} coordinating residues in each Mg^{2+} binding site, Asp99, Asn172, Glu374 and Glu399, should come from the same Slo1 protein, *i.e.*, the BK channel forms intra-subunit Mg^{2+} binding sites. To examine this prediction, we mixed single mutations D99R and E374R in 1:1 ratio (Fig. 6b), and tested their Mg^{2+} sensitivity (Fig. 6c-e). These mixed single mutants form heterotetrameric channels when expressed in *Xenopus* oocytes with various stoichiometry (Supplementary Fig. 2a). Since each of the single mutation in a Mg^{2+} binding site is sufficient to abolish Mg^{2+} binding (Fig. 6c, d), if intra-subunit Mg^{2+} binding sites are formed, all four sites of a channel should be completely destroyed no matter what the stoichiometry is for the heterotetrameric channels (Supplementary Fig. 2a). Therefore, no Mg^{2+} sensitivity of any mixed channels should be observed. However, when we mixed D99R and E374R in 1:1 ratio, the channels exhibited a -14.8±1.2 mV (n=9), Mg^{2+}-induced *G-V* shift (Fig. 6c, e). This residual Mg^{2+} sensitivity is significantly different ($p<0.001$) from D99R single mutant (n=13), E374R single mutant (n=11), or D99R E374R double mutant channels (n=7), all of which completely abolish Mg^{2+} sensing (Fig. 7a).

To explain this phenomenon, we postulated an inter-subunit Mg^{2+} binding site model, in which Asp99 from the VSD and Glu374 from the cytoplasmic domain are from neighboring subunits (Fig. 7b and Supplementary Fig. 2b). According to this model, some D99R:E374R heterotetrameric channels may contain one or two intact Mg^{2+} binding site(s). If each binding site is assumed to make an equal contribution to channel activation independently, the model predicts a -13.3 mV shift (25% of that of the WT channel) in the *G-V* relation of the mixed channels in the presence of 10 mM $[Mg^{2+}]_i$ (Supplementary Fig. 2b and

METHODS). Our experimental observation is consistent with this model prediction (Fig. 7a). Current amplitudes of D99R channels, E374R channels and D99R:E374R mixed channels were comparable in these experiments (Fig. 6c), indicating that the expression efficiency of D99R and E374R are similar, and hence the mix of D99R and E374R is at a 1:1 ratio.

Similarly, for the 1:1 mixture of N172R:E374R (Fig. 7a, inset), 10 mM $[Mg^{2+}]_i$ also induced a *G-V* shift of -18.3±1.7 mV (Fig. 7a, n=6), suggesting that in the Mg^{2+} binding site, Asn172 and Glu374 also come from neighboring subunits. Contrary to the mix of mutations that are in different domains, the mix of mutations that are in the same domain, i.e., D99R:N172R (n=12) in the VSD or E374R:E399C (n=12) in the cytoplasmic domain (Fig. 7a, inset), did not rescue any Mg^{2+} sensitivity (Fig. 7a). This result rules out the possibility that the rescued Mg^{2+} sensitivity is due to some non-specified artifacts that might have been derived from mixing different mutations. Based on all these experiments, we conclude that Asp99 and Asn172 from the VSD and Glu374 and Glu399 from the cytoplasmic domain form an inter-domain and inter-subunit Mg^{2+} binding site (Fig. 7c).

DISCUSSION

Our results illustrate that Mg^{2+} is coordinated at the interface between the VSD and the cytoplasmic domain to activate Slo1 BK channels. Side chains from Asp99/Asn172 in the VSD and Glu374/Glu399 in the cytoplasmic domain form the putative Mg^{2+} binding site. This coordination scheme positions Mg^{2+} close to the S4 voltage sensor and enables an electrostatic interaction between the bound Mg^{2+} with Arg213 in S4 to affect the movements of the VSD, thereby activating the channel14. Interestingly, the mixture experiments shown in Figure 6 and 7 suggest that the putative Mg^{2+} binding site of BK channels is formed between neighboring subunits. Thus, the VSD and the cytoplasmic domain from different subunits would interact during channel gating.

This special inter-domain and inter-subunit arrangement of the putative Mg^{2+} binding site provides valuable structural and functional information about BK channels. First, the two sensory domains, the VSD and the cytoplasmic domain, are close to each other and may interact intimately during channel gating. According to the octahedral geometry of Mg^{2+} binding, the Mg^{2+} ligands must be positioned within 5 to 6 Å from each other when Mg^{2+} binds to the site23 (Fig. 1c, inset). Thus, the top surface of the cytoplasmic domain may make close contact with the intracellular face of the VSD. Our recent study on the electrostatic interaction between Arg213 in S4 and the positive charge on residue 397 suggests that these two positive charges are about 9 Å apart14, supporting our current finding on the Mg^{2+} binding site and the proximity between these two sensory domains. The disulfide bond between Cys99 and Cys397 (Fig. 3) and the ability of N172D to substitute mutations of other Mg^{2+} ligands to bind Mg^{2+} (Fig. 5c) further suggest that these two sensory domains interact closely at their interface. However, it is not clear whether there are other places besides the Mg^{2+} binding site where these two sensory domains interact with each other to regulate channel gating. Second, the formation of inter-subunit Mg^{2+} binding sites suggests that the VSD of one subunit is packed right on top of the cytoplasmic domain from the neighboring subunit (Fig. 7). Such a structural arrangement does not agree with the

prediction of the quaternary structure model based on the superposition of the Kv1.2 and MthK structures (Fig. 6a). This result indicates that although the VSD and the cytoplasmic RCK1 domain of BK channels may adopt a similar tertiary structure as that of Kv1.2 and MthK channels3,8,12,14,19-21, the packing of VSD or the cytoplasmic domain relative to the pore domain may differ from that of Kv1.2 or MthK. Such a difference in the quaternary structure may be the result of the unique S0 transmembrane segment31 and the long S0-S1 loop in the TM domain (Fig. 2a) besides the common VSD (S1-S4) that is found in other Kv channels, as well as the intimate interactions between the VSD and the cytoplasmic domain of BK channels. Since the packing of the voltage sensor and the cytoplasmic ligand sensor relative to the pore domain may influence the energetic coupling between these sensors and the activation gate, it may contribute to the unique functional properties of the BK channel, such as the allosteric mechanism of voltage- and Ca^{2+}-dependent gating26,32.

Based on a quantum chemistry calculation23 of the free energy of successive water-exchange reactions in Mg^{2+} complexes, Dudev and Lim concluded that neutral carbonyl group(s) (in the case of the mSlo1 BK channel, Asn172) can coordinate Mg^{2+} when Mg^{2+} is already bound to up to three negatively charged carboxylate groups (Asp99, Glu374 and Glu399 in the mSlo1 BK channel). Under this composition of a Mg^{2+} binding site, Mg^{2+} cannot exchange all its first-shell water molecules for protein ligands. In our study, we did not find any other residue than Asp99, Asn172, Glu374, and Glu399 that contributes a potential ligand to Mg^{2+} coordination. Our observation is consistent with this theoretical prediction. Therefore, another two coordinates of the Mg^{2+} site may come from water molecules. It is also possible that additional water molecule(s) may directly coordinate Mg^{2+} such that some of the side chain(s) among Asp99, Asn172, Glu374, and Glu399 may serve as second shell ligand(s) to stabilize these water molecules in the first coordination shell33.

According to thermodynamic principles, Mg^{2+} binds to the channel with a higher affinity in the open state of the channel than in the closed state, thus facilitating channel opening24,34,35. The identification of the inter-domain formation of the Mg^{2+} binding site in this study provides a possible mechanism to explain the increase of Mg^{2+} binding affinity during channel opening. Recent studies on Mg^{2+}-dependent activation indicate that the electrostatic interaction between Mg^{2+} and the VSD depends on channels opening, suggesting that a relative movement between the cytoplasmic domain and the VSD may occur during channel gating14,27. This relative movement may induce rearrangement of the relative orientation of Asp99, Asn172, Glu374 and Glu399, thereby resulting in optimal coordination and higher Mg^{2+} binding affinity in the open state.

METHODS

Mutagenesis and expression

All channel constructs were made from the mbr5 clone of the mouse Slo1 BK (mSlo1) by using PCR with Pfu polymerase (Stratagene, La Jolla, CA). The PCR-amplified regions of all mutants were verified by sequencing. RNA was transcribed in vitro with T3 polymerase (Ambion, Austin, TX). We injected 0.05-50 ng (for macroscopic currents) or 150-250 ng (for gating currents) of RNA into each *Xenopus* laevis oocyte 2-6 days before recording. For the mixture experiments, the mRNAs of two single mutants were mixed with 1:1 ratio; the

same amount of mRNA of each single mutant was also injected as a control to monitor the expression rate.

Electrophysiology

Ionic currents were recorded with inside-out patches using Axopatch 200-B patch-clamp amplifier (Axon Instruments, Union City, CA) and Pulse acquisition software (Pulse; Heka Electronik, Lambrecht/Pfalz, Germany)12. The pipette solution contains (mM): 140 potassium methanesulfonic acid, 20 HEPES, 2 KCl, 2 $MgCl_2$, pH 7.2. The basal internal solution contains (mM): 140 potassium methanesulfonic acid, 20 HEPES, 2 KCl, pH 7.2. $MgCl_2$ was added to the internal solution (with 5 mM EGTA) to give the 10 mM free $[Mg^{2+}]_i$. A sewer pipe flow system was used to perfuse the internal solution on the cytoplasmic face of the patch.

Gating currents were recorded with inside-out patches25. The pipette solution contains (in mM): 127 tetraethylammonium (TEA) hydroxide, 125 methanesulfonic acid, 2 HCl, 2 $MgCl_2$, 20 HEPES, pH 7.2. The internal solution contains (in mM): 141 N-methyl-D-glucamine (NMDG), 135 methanesulfonic acid, 6 HCl, 20 HEPES, 5 EGTA, pH 7.2. Gating currents of the same patch were first recorded in the absence of Mg^{2+}, and then 2.5 M $MgCl_2$ stock solution was added to the distal place of the bath stage (to avoid the disturbance of the seal of the patch), followed by a 6 min equilibration period to reach the target 10 mM before recording.

Voltage commands were filtered at 20 kHz with an eight-pole Bessel filter (Frequency Devices, Haverhill, MA) to prevent the saturation of fast capacitive transients25. Data were sampled at 100 kHz with an 18 bit A/D converter (ITC-18; Instrutech, Port Washington, NY) and filtered at 10 kHz with Axopatch's internal filter. Capacitive transients and leak currents were subtracted using a P/5 protocol with a holding potential of -120 mV. All chemicals were obtained from Sigma-Aldrich Corp. (St Louis, MO, USA) unless otherwise noted.

Chemical Modification

10 mM dithiothreitol (DTT) was freshly made before each experiment. The inside-out patches were recorded first, followed by a 10-min treatment, and then were recorded again to see the DTT effect. [2-(trimethylammonium)ethyl] methanethiosulfonate bromide (MTSET) was purchased from Toronto Research Chemicals. An aliquot of 100 mM MTSET stock solution was thawed and diluted 500-fold into the basal internal solution immediately before use. In ionic current recordings, currents were recorded after 2.5 min of MTSET treatment and 0.5 min of washing of the intracellular side of patches.

Data Analysis and the model for inter-domain Mg^{2+} binding site

Relative conductance was determined by measuring macroscopic tail current amplitudes at -80 mV. The conductance-voltage (*G*-*V*) relations of the WT and mutant channels were fitted with the Boltzmann equation:

$$G/G_{Max}=1/(1+exp(-ze(V-V_{1/2})/kT)) \quad (1)$$

where, z is the number of equivalent gating charges, $V_{1/2}$ is the voltage for channel in half activation, e is the elementary charge, k is Boltzmann's constant and T is the absolute temperature. Each *G-V* curve was obtained from n = 5-24 patches. Error bars represent the standard error of mean in all figures.

Supplementary Figure 2b illustrates all the combinations of D99R:E374R mixture in 1:1 ratio with a binomial distribution, assuming that the Mg^{2+} binding site is formed by Asp99 and Glu374 from neighboring subunits. Each BK channel expressed from this mix contains n subunits of E374R ($n \leq 4$) and (4-n) subunits of D99R. Thus, the probability of n = 0, 1, 2, 3, and 4 will be 0.0625, 0.25, 0.375, 0.25 and 0.0625, respectively. For n = 0 or 4, the channel is formed by either E374R or D99R so that there is no chance to form any intact binding site. For n = 1 or 3, there are four different arrangements of the channels, each of which is formed by one E374R and three D99R or vice versa, so that there is always one intact binding site. For n = 2, there are six different arrangements of the channels, each of which is formed by two E374R and two D99R. Among these six arrangements, four contain one intact binding site and two contain two intact binding sites. Therefore, the probability of forming a channel with 0, 1 and 2 intact binding sites is 0.125, 0.75 and 0.125, respectively. If each intact Mg^{2+} binding site makes an equal contribution to channel activation independently (25% of total Mg^{2+} sensing), the remaining Mg^{2+} sensitivity is:

$$(0.75\times 0.25\times 1+0.125\times 0.25\times 2)\times(-53.2)=0.25\times(-53.2)=-13.3\,mV,$$

where -53.2 is the Mg^{2+} sensitivity contributed by the Glu374/Glu399 site of WT channels from 0 to 10 mM $[Mg^{2+}]_i$.

Statistics were performed using SigmaStat 3.5 (Systat Software, Inc., San Jose, CA); Student's *t*-test or One-Way ANOVA with an all-pairwise multiple comparison procedure (Tukey test) was performed. A p value of <0.05 was considered significant.

Structural Model

The structure of Mg^{2+} binding site of the mSlo1 channel was generated based on the crystal structure of the MthK channel by using the PyMol molecular graphics system (http://www.pymol.org).

Supplementary Material

Refer to Web version on PubMed Central for supplementary material.

Acknowledgments

We thank Lei Hu for calculations of Mg^{2+} sensitivity according to the model of inter-subunit Mg^{2+} binding site. We thank Chris Lingle, Lawrence Salkoff, and Lei Hu for critical discussion. The mSlo1 clone was kindly provided by Lawrence Salkoff (Washington University, St. Louis, MO). Frank Horrigan (Baylor College of Medicine, Houston, TX) kindly provided Y163K mutant mSlo1 cDNA. This work was supported by National Institutes of

Health Grant R01-HL70393 and National Science Foundation of China Grant 30528011 (J.C.). J.C. is an Associate Professor of Biomedical Engineering on the Spencer T. Olin Endowment.

References

1. Hille, B. Ion channels of excitable membranes. Sinauer; Sunderland, MA: 2001.
2. Long SB, Campbell EB, Mackinnon R. Voltage sensor of Kv1.2: structural basis of electromechanical coupling. Science. 2005; 309:903–8. [PubMed: 16002579]
3. Jiang Y, Lee A, Chen J, Cadene M, Chait BT, MacKinnon R. Crystal structure and mechanism of a calcium-gated potassium channel. Nature. 2002; 417:515–22. [PubMed: 12037559]
4. Miyazawa A, Fujiyoshi Y, Unwin N. Structure and gating mechanism of the acetylcholine receptor pore. Nature. 2003; 423:949–55. [PubMed: 12827192]
5. Latorre R, Brauchi S. Large conductance Ca^{2+}-activated K^+ (BK) channel: activation by Ca^{2+} and voltage. Biol Res. 2006; 39:385–401. [PubMed: 17106573]
6. Magleby KL. Gating mechanism of BK (Slo1) channels: so near, yet so far. J Gen Physiol. 2003; 121:81–96. [PubMed: 12566537]
7. Salkoff L, Butler A, Ferreira G, Santi C, Wei A. High-conductance potassium channels of the SLO family. Nat Rev Neurosci. 2006; 7:921–931. [PubMed: 17115074]
8. Hou S, Xu R, Heinemann SH, Hoshi T. Reciprocal regulation of the Ca^{2+} and H^+ sensitivity in the SLO1 BK channel conferred by the RCK1 domain. Nat Struct Mol Biol. 2008; 15:403–10. [PubMed: 18345016]
9. Hou S, Xu R, Heinemann SH, Hoshi T. The RCK1 high-affinity Ca^{2+} sensor confers carbon monoxide sensitivity to Slo1 BK channels. Proc Natl Acad Sci U S A. 2008; 105:4039–43. [PubMed: 18316727]
10. Tang XD, Xu R, Reynolds MF, Garcia ML, Heinemann SH, Hoshi T. Haem can bind to and inhibit mammalian calcium-dependent Slo1 BK channels. Nature. 2003; 425:531–5. [PubMed: 14523450]
11. Zeng XH, Xia XM, Lingle CJ. Divalent cation sensitivity of BK channel activation supports the existence of three distinct binding sites. J Gen Physiol. 2005; 125:273–86. [PubMed: 15738049]
12. Shi J, Krishnamoorthy G, Yang Y, Hu L, Chaturvedi N, Harilal D, Qin J, Cui J. Mechanism of magnesium activation of calcium-activated potassium channels. Nature. 2002; 418:876–80. [PubMed: 12192410]
13. Xia XM, Zeng X, Lingle CJ. Multiple regulatory sites in large-conductance calcium-activated potassium channels. Nature. 2002; 418:880–4. [PubMed: 12192411]
14. Yang H, Hu L, Shi J, Delaloye K, Horrigan FT, Cui J. Mg^{2+} mediates interaction between the voltage sensor and cytosolic domain to activate BK channels. Proc Natl Acad Sci U S A. 2007; 104:18270–5. [PubMed: 17984060]
15. Ledoux J, Werner ME, Brayden JE, Nelson MT. Calcium-activated potassium channels and the regulation of vascular tone. Physiology (Bethesda). 2006; 21:69–78. [PubMed: 16443824]
16. Toro L, Wallner M, Meera P, Tanaka Y. Maxi-K_{Ca}, a Unique Member of the Voltage-Gated K Channel Superfamily. News Physiol Sci. 1998; 13:112–117. [PubMed: 11390773]
17. Fettiplace R, Fuchs PA. Mechanisms of hair cell tuning. Annu Rev Physiol. 1999; 61:809–34. [PubMed: 10099711]
18. Du W, Bautista JF, Yang H, Diez-Sampedro A, You SA, Wang L, Kotagal P, Luders HO, Shi J, Cui J, Richerson GB, Wang QK. Calcium-sensitive potassium channelopathy in human epilepsy and paroxysmal movement disorder. Nat Genet. 2005; 37:733–8. [PubMed: 15937479]
19. Ma Z, Lou XJ, Horrigan FT. Role of Charged Residues in the S1-S4 Voltage Sensor of BK Channels. J Gen Physiol. 2006; 127:309–328. [PubMed: 16505150]
20. Jiang Y, Pico A, Cadene M, Chait BT, MacKinnon R. Structure of the RCK domain from the E. coli K^+ channel and demonstration of its presence in the human BK channel. Neuron. 2001; 29:593–601. [PubMed: 11301020]
21. Fodor AA, Aldrich RW. Statistical limits to the identification of ion channel domains by sequence similarity. J Gen Physiol. 2006; 127:755–66. [PubMed: 16735758]

22. Yang H, Hu L, Shi J, Cui J. Tuning Magnesium Sensitivity of BK Channels by Mutations. Biophys J. 2006; 91:2892–900. [PubMed: 16877509]
23. Dudev T, Lim C. Principles governing Mg, Ca, and Zn binding and selectivity in proteins. Chem Rev. 2003; 103:773–88. [PubMed: 12630852]
24. Hu L, Yang H, Shi J, Cui J. Effects of Multiple Metal Binding Sites on Calcium and Magnesium-dependent Activation of BK Channels. J Gen Physiol. 2006; 127:35–50. [PubMed: 16344323]
25. Horrigan FT, Aldrich RW. Allosteric voltage gating of potassium channels II. Mslo channel gating charge movement in the absence of Ca^{2+} J Gen Physiol. 1999; 114:305–36. [PubMed: 10436004]
26. Horrigan FT, Aldrich RW. Coupling between voltage sensor activation, Ca^{2+} binding and channel opening in large conductance (BK) potassium channels. J Gen Physiol. 2002; 120:267–305. [PubMed: 12198087]
27. Horrigan FT, Ma Z. Mg^{2+} enhances voltage sensor/gate coupling in BK channels. J Gen Physiol. 2008; 131:13–32. [PubMed: 18166624]
28. Hazes B, Dijkstra BW. Model building of disulfide bonds in proteins with known three-dimensional structure. Protein Eng. 1988; 2:119–25. [PubMed: 3244694]
29. Flynn GE, Zagotta WN. Conformational changes in S6 coupled to the opening of cyclic nucleotide-gated channels. Neuron. 2001; 30:689–98. [PubMed: 11430803]
30. Long SB, Campbell EB, Mackinnon R. Crystal structure of a mammalian voltage-dependent Shaker family K^+ channel. Science. 2005; 309:897–903. [PubMed: 16002581]
31. Wallner M, Meera P, Toro L. Determinant for beta-subunit regulation in high-conductance voltage-activated and Ca^{2+}-sensitive K^+ channels: an additional transmembrane region at the N terminus. Proc Natl Acad Sci U S A. 1996; 93:14922–7. [PubMed: 8962157]
32. Cox DH, Cui J, Aldrich RW. Allosteric gating of a large conductance Ca-activated K^+ channel. J Gen Physiol. 1997; 110:257–81. [PubMed: 9276753]
33. Dudev T, Lin YL, Dudev M, Lim C. First-second shell interactions in metal binding sites in proteins: a PDB survey and DFT/CDM calculations. J Am Chem Soc. 2003; 125:3168–80. [PubMed: 12617685]
34. Shi J, Cui J. Intracellular Mg^{2+} enhances the function of BK-type Ca^{2+}-activated K^+ channels. J Gen Physiol. 2001; 118:589–606. [PubMed: 11696614]
35. Zhang X, Solaro CR, Lingle CJ. Allosteric regulation of BK channel gating by Ca^{2+} and Mg^{2+} through a nonselective, low affinity divalent cation site. J Gen Physiol. 2001; 118:607–36. [PubMed: 11696615]
36. Zhang G, Horrigan FT. Cysteine modification alters voltage- and Ca^{2+}-dependent gating of large conductance (BK) potassium channels. J Gen Physiol. 2005; 125:213–36. [PubMed: 15684095]

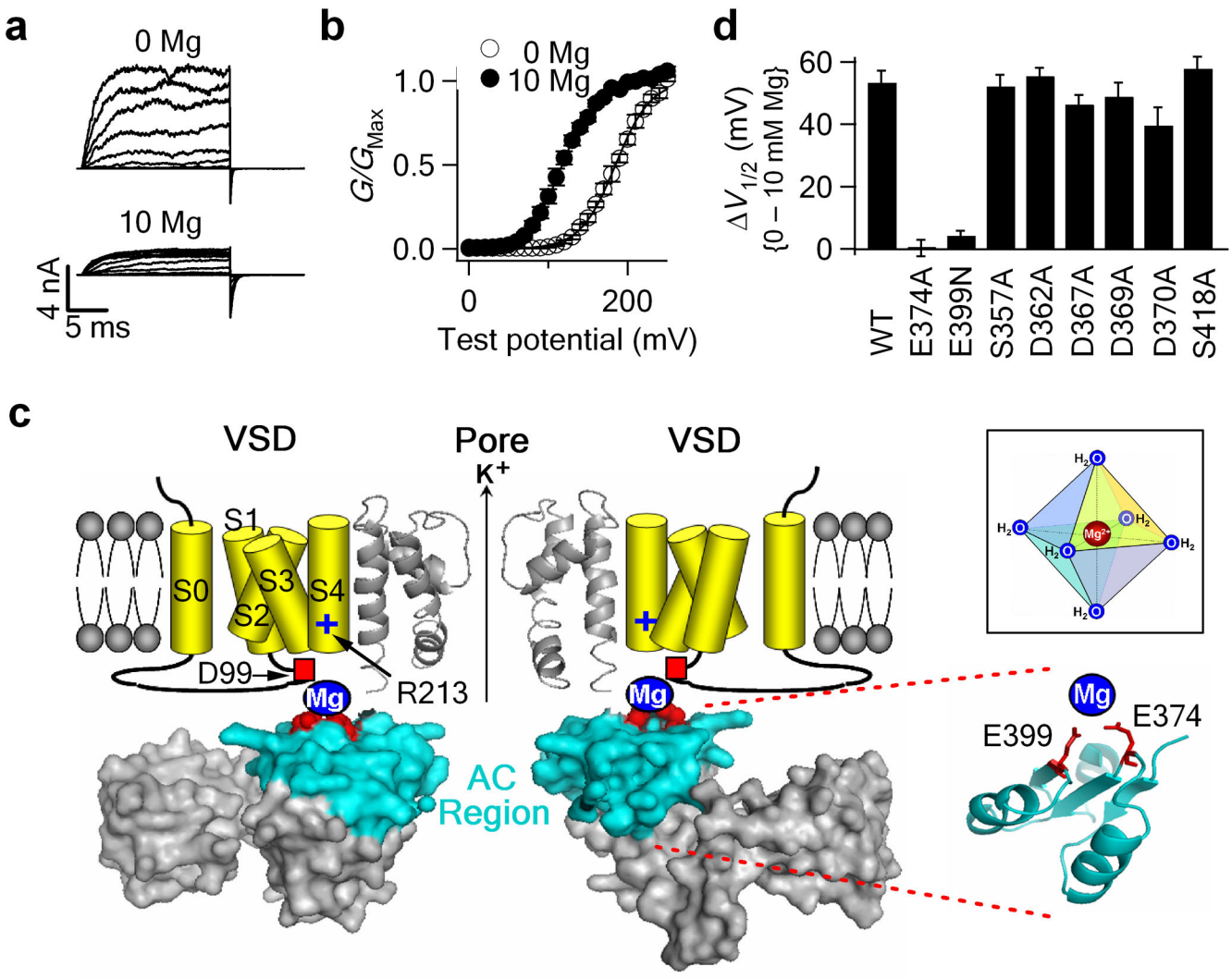

Figure 1.

Mg^{2+} coordinates in the cytoplasmic domain of the mSlo1 channel. (**a**,**b**) Representative macroscopic current traces (**a**) and mean *G-V* relationship (**b**) for WT channels in 0 and 10 mM $[Mg^{2+}]_i$. Testing potentials were from -20 to 240 mV with 20-mV increments. Both holding and repolarizing potentials were -80 mV. The smooth curves in (**b**) represent Boltzmann fits. (**c**) BK channel model. The pore domain and the cytoplasmic RCK1 domain is based on the MthK crystal structure (PDB ID: 1LNQ)3. Transmembrane S0-S4 segments are depicted as cartoons. Only two opposite subunits are shown for clarity. Two putative Mg^{2+} binding residues (Glu374 and Glu399, red spheres) are located in the AC region (cyan). (Inset) Mg^{2+} binding site is predominantly formed by six oxygen-containing ligands with an octahedral geometry. (**d**) Shifts of the *G-V* relation caused by 10 mM $[Mg^{2+}]_i$ for the Ala mutations of the oxygen-containing residues in the AC region. When the putative Mg^{2+} binding residues (Glu374 and Glu399) were destroyed, 10 mM $[Mg^{2+}]_i$ still shifts *G-V* relation to more negative voltages by about 14 mV due to Mg^{2+} binding to a very low affinity Mg^{2+} site24. This effect can be mathematically subtracted to obtain the contribution of the Glu374/Glu399 site to Mg^{2+} sensing. Thus, in all figures in this study, mean *G-V*

relationships show the observed *G-V* shifts induced by 10 mM $[Mg^{2+}]_i$; while the *G-V* shifts in all bar graphs represent the contribution of the Glu374/Glu399 site after 14.0 mV subtraction. Error bars represent s.e.m.

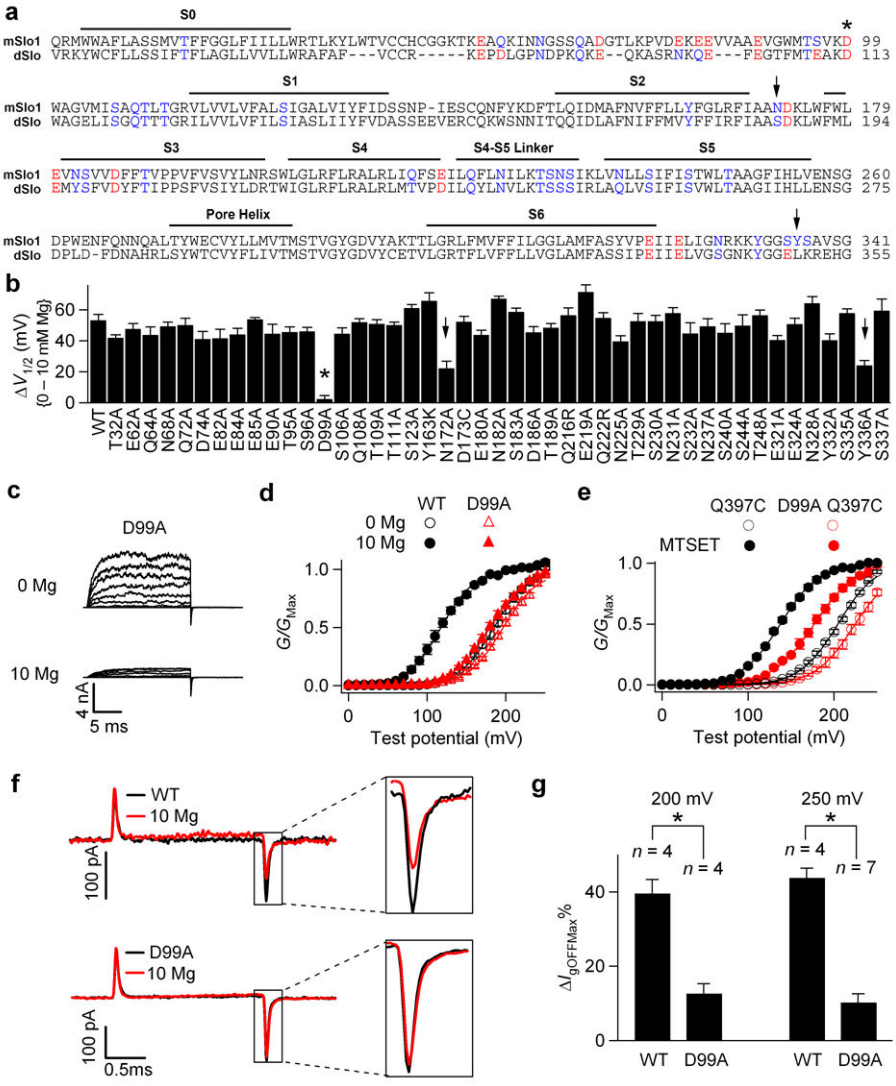

Figure 2.

D99A abolishes Mg^{2+} sensitivity by preventing Mg^{2+} binding. (**a**) Sequence alignment of the membrane-spanning (TM) domain in mSlo1 and dSlo channels. Mutations of the oxygen-containing residues that are conserved between mSlo1 and dSlo and potentially face cytosol (red and blue colors) were tested. mSlo1: (mouse, GI: 347143); dSlo: (drosophila, GI: 115311626). (**b**) Shifts of the *G-V* relationship induced by 10 mM $[Mg^{2+}]_i$ for WT and the mutations. (**c**) Macroscopic current traces of D99A in 0 and 10 mM $[Mg^{2+}]_i$. Testing potentials were from -20 to 240 mV with 20-mV increments. Both holding and repolarizing potentials were -80 mV. (**d**) *G-V* relationship for WT and D99A. (**e**) Mean *G-V* relationship of Q397C and D99A Q397C channels before (hollow) and after (filled) 200 μM MTSET treatment. For all the experiments with MTSET treatment in this study, C430A was used as background to remove the endogenous MTSET effect on channel activation14,36. (**f**) Gating current (I_g) traces for WT (upper panel) and D99A mutant (lower panel) channels with (red) and without (black) 10 mM $[Mg^{2+}]_i$ in response to a 2-ms, 250 mV depolarizing pulse. I_g traces of the same patch were first recorded in the absence of Mg^{2+}, and then 10 mM

$[Mg^{2+}]_i$. (**g**) Effects of 10 mM $[Mg^{2+}]_i$ on the reduction of peak OFF gating currents ($I_{gOFFMax}$) in response to 2-ms, 200 mV or 250 mV depolarizing pulses.$\Delta I_{gOFFMax}\% = (I_{gOFFMax(0Mg)} - I_{gOFFMax(10Mg)})/I_{gOFFMax(0Mg)}$. * indicates $p \leq 0.001$.

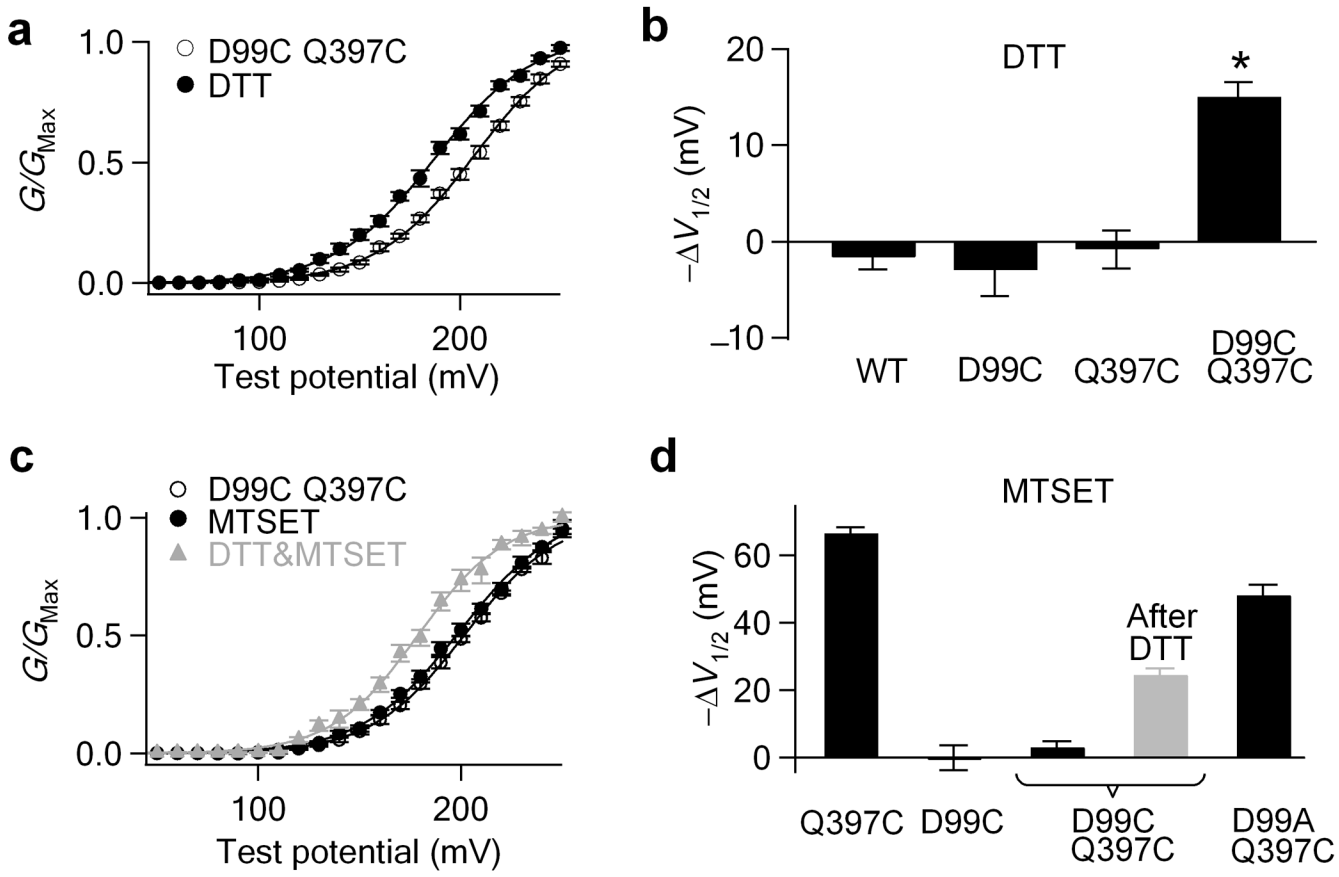

Figure 3.

Asp99 is spatially close to the cytoplasmic part of the Mg^{2+} binding site. (**a**, **b**)Shifts of the *G-V* relationship induced by 10 mM DTT in 0 $[Ca^{2+}]_i$ and $[Mg^{2+}]_i$. * indicates $p<0.001$. (**c**) Mean *G-V* relationship of D99C Q397C mutant channels before and after 200 μM MTSET or sequential DTT-MTSET (grey) treatment in 0 $[Mg^{2+}]_i$. (**d**) *G-V* shifts induced by MTSET treatments, suggesting the disulfide formation between Cys99 and Cys397.

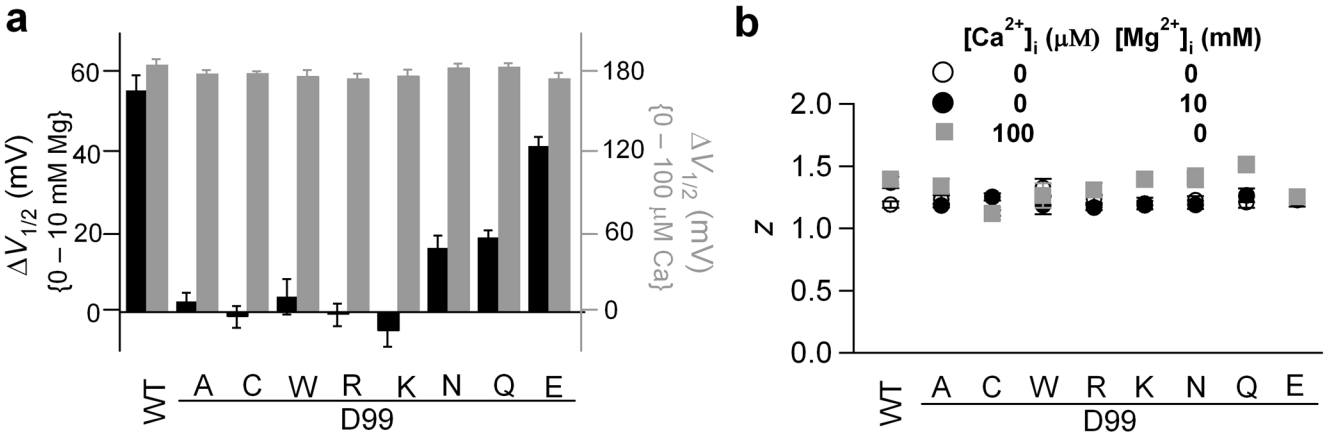

c

```
mSlo1   RTLKYLWTVCCHCGGKT-KEAQKIN-NGSSQ-ADGTLKPVDEK---EEVVAAEVGWMTSVKDWAGVMISAQTLTGR 113
hSlo    RTLKYLWTVCCHCGGKT-KEAQKIN-NGSSQ-ADGTLKPVDEK---EEAVAAEVGWMTSVKDWAGVMISAQTLTGR 178
gSlo    RTLKYLWTVCCHCGVKN-KEAQKINGGGDTQ-ADGACKPTDEK---EENVAAEVGWMTSVKDWAGVMISAQTLTGR 137
tSlo    RTLKYLWTVCCHCGVKN-KEAQKINAGGGNQ-ADGTCKPTDEK---EETVAAEVGWMTSVKDWAGVMISAQTLTGR 114
xSlo    RTFKYLWTVCCHCGGKN-KEAQKVVNVASSQVTDGDYKPTDDK---EEVGVAEVGWMTSVKDWAGVMISAQTLTGR 146
dSlo    RAF---AFVCCRK------EPDLGP-------NDPKQKEQKAS---RNKQEFEGTFMTEAKDWAGELISGQTTTGR 127
cSlo    RVVTH---LCCQRREKEFVEPIPAPEAVQINMNGSKHAPSETDPFLKQQEEKHLGWMTEAKDWAGELISGQSLTGR 139
```

Figure 4.

Side chain carboxylate or carbonyl group of residue 99 is required for Mg^{2+} coordination. (**a**) *G-V* shifts induced by 10 mM $[Mg^{2+}]_i$ (black) and by 100 μM $[Ca^{2+}]_i$ (grey) for Asp99 mutations. (**b**) Equivalent gating charge *z* of Asp99 mutations. (**c**) Sequence alignment of the S0-S1 linker from various spices: mouse (mSlo1, GI: 347143), human (hSLO, GI: 46396283), chicken (gSlo, GI:46396408), turtle (tSlo, GI:82224841), frog (xSlo, GI: 46396489), drosophila (dSlo, GI: 115311626), nematode (cSlo, GI:46396994).

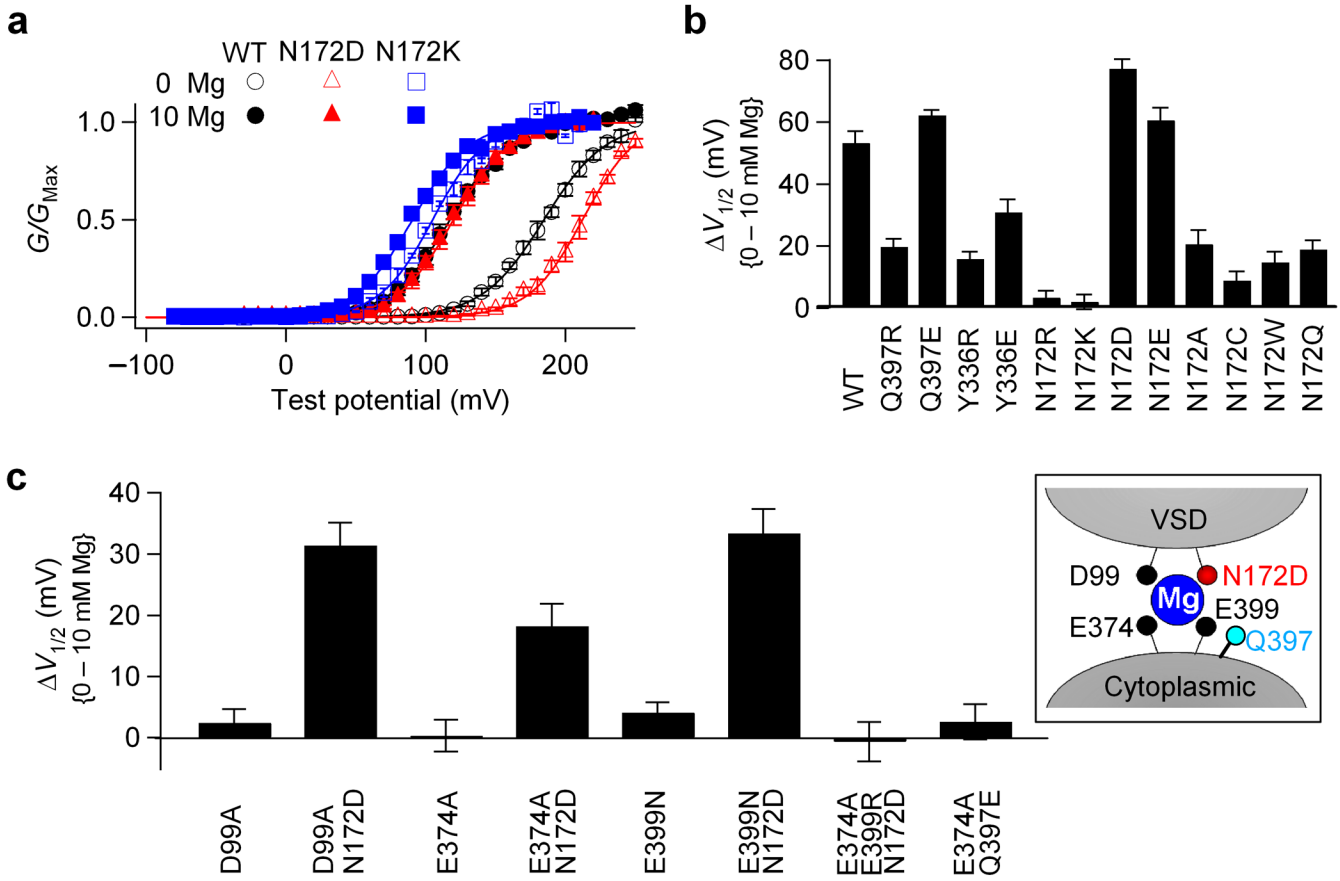

Figure 5.

Asn172 may contribute to Mg^{2+} coordination. (**a**) Mean *G-V* relationship of WT, N172D and N172K mutant channels in 0 and 10 mM $[Mg^{2+}]_i$. (**b**) Shifts of the *G-V* relationship caused by 10 mM $[Mg^{2+}]_i$ for WT and Gln397, Tyr336, and Asn172 mutations. (**c**) Shifts of the *G-V* relationship caused by 10 mM $[Mg^{2+}]_i$. Inset, N172D may substitute other putative Mg^{2+} coordinates to enable Mg^{2+} binding.

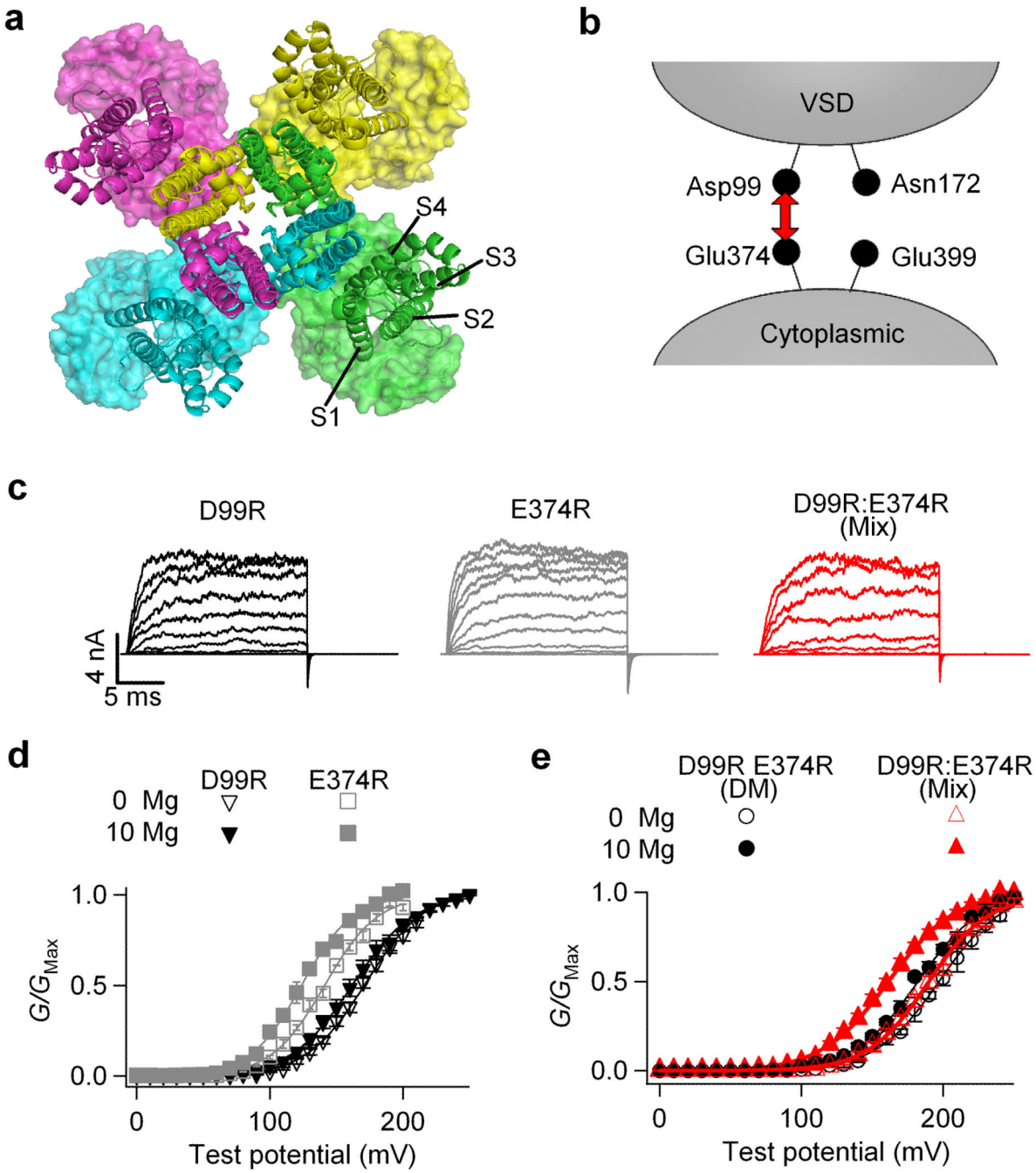

Figure 6.

Asp99 and Glu374 in a Mg^{2+} binding site are not from the same subunit. (**a**)Superposition of Kv1.2 (ribbons, PDB ID: 2A79)30 and MthK (surface, PDB ID: 1LNQ)3 channel structures by aligning their selectivity filter regions. For clarity, the T1 domains of the Kv1.2 structure and the RCK2 domains of the MthK structure were not shown. Different colors represent four subunits. (**b**) Experimental design for mixing D99R and E374R mutations. (**c**) Representative current traces of D99R, E374R and mixed D99R:E374R (1:1) channels. (**d**) Mean *G-V* relationship of D99R and E374R channels. The small shift in *G-V* relations is

largely due to Mg^{2+} binding to another low affinity Mg^{2+} site24 (**e**) Mean *G-V* relationship of the D99R E374R double mutant (DM) and D99R:E374R mixed (1:1) channels.

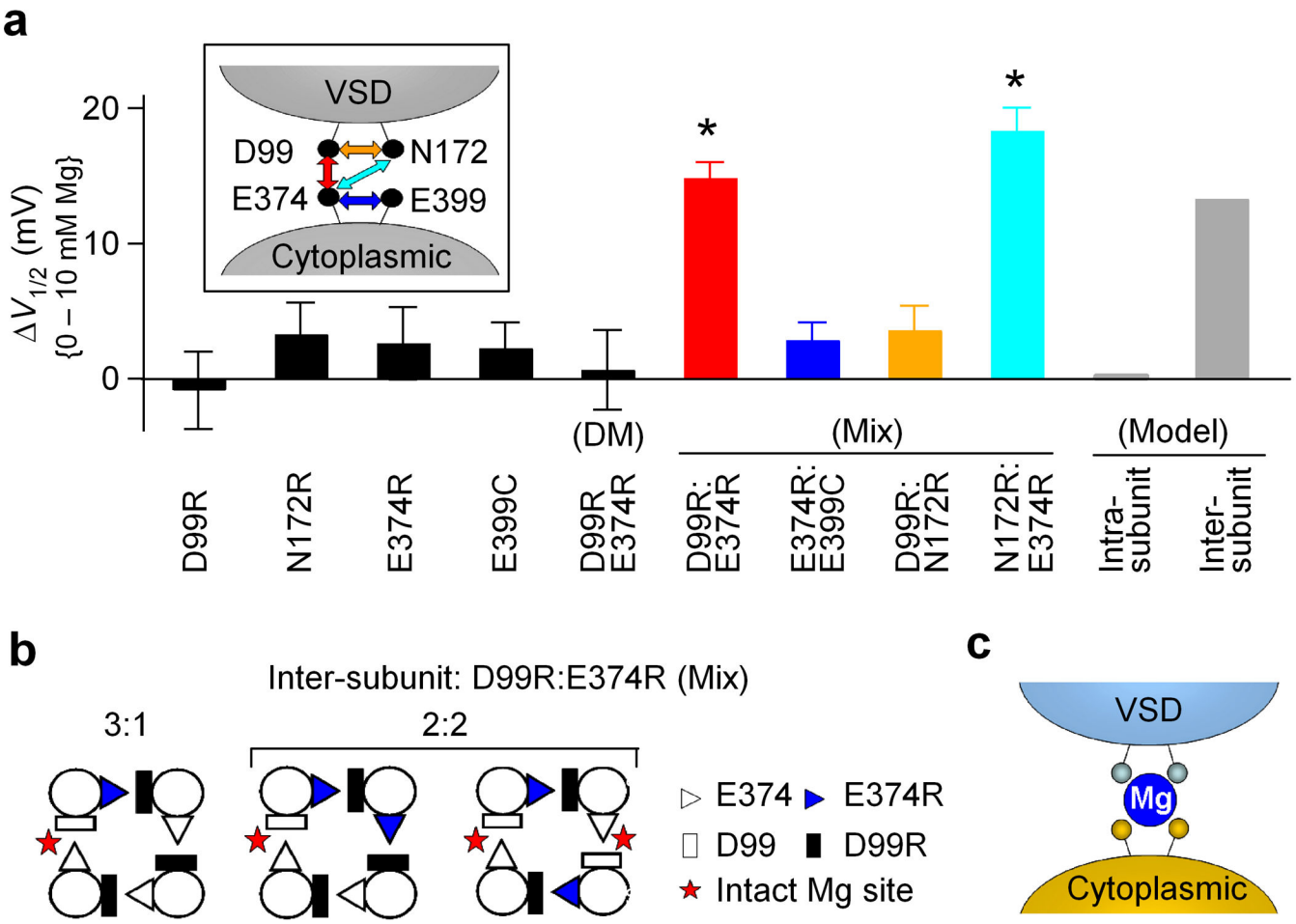

Figure 7.

Asp99/Asn172 and Glu374/Glu399 may come from neighboring subunits to form a Mg^{2+} binding site. (**a**) Shifts of the *G-V* relationship caused by 10 mM $[Mg^{2+}]_i$ for various single and combinations of mutations. Different mixed mutations are color coded as the arrows shown in the inset. All the mixtures have a mRNA ratio of 1:1. Model prediction was calculated based on a binomial distribution (See Methods). * indicates $p<0.001$. (**b**) Intact Mg^{2+} binding sites can form from mixed mutations based on inter-subunit formation of the Mg^{2+} binding sites. (**c**) Cartoon illustrating inter-domain and inter-subunit formation of the Mg^{2+} binding site.